Supplementary Information: Varying patterns of association between cortical large-scale networks and subthalamic nucleus activity in Parkinson's Disease

Oliver Kohl[1], Chetan Gohil[2], Matthias Sure[1], Alfons Schnitzler[1,3], Esther Florin[1]

Table of Contents

Supplementary Figure 1 – Motor cortical beta power and sensorimotor network fractional occupancy are reduced in PD compared to HCs

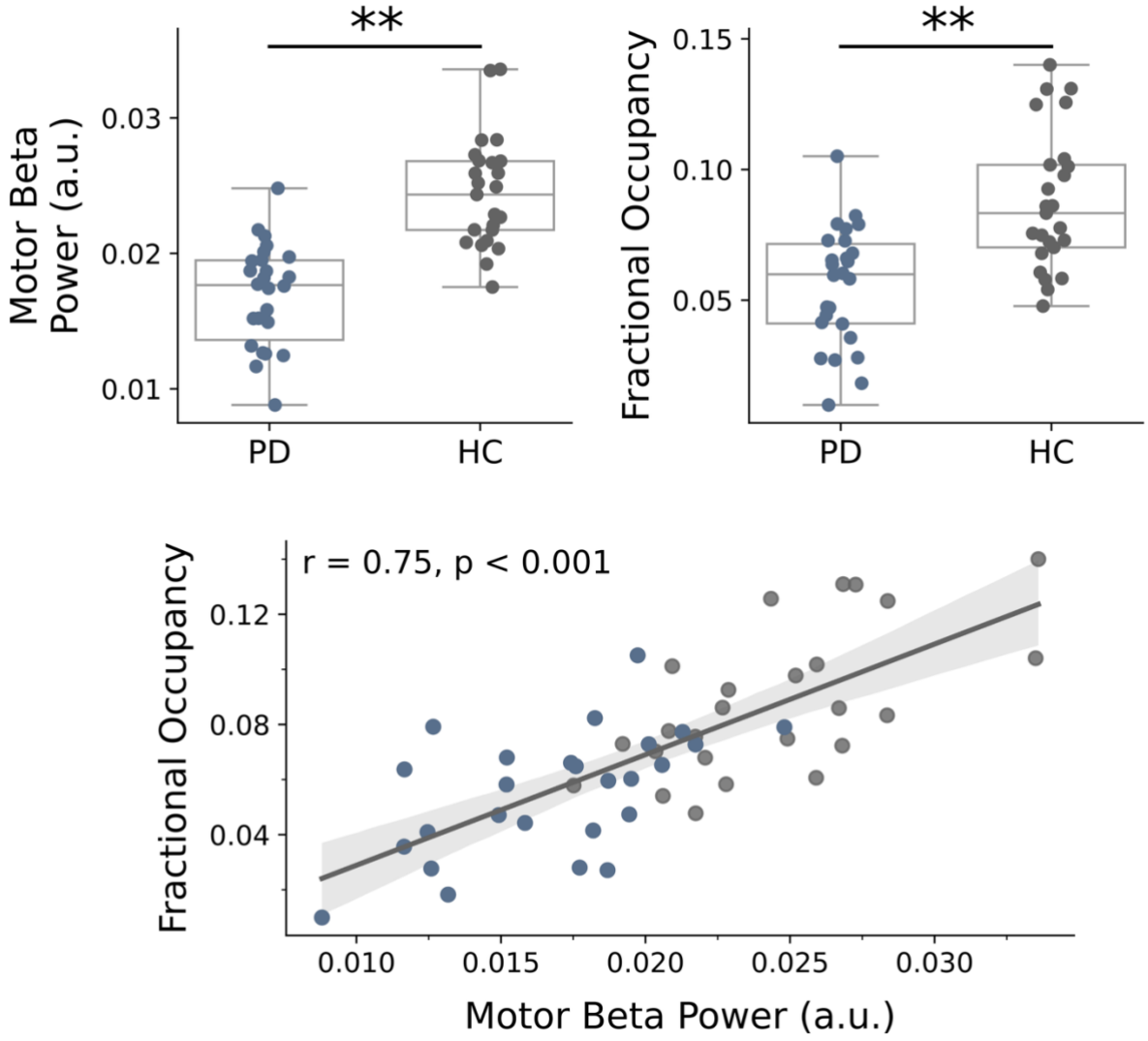

Supplementary Figure 1. Reductions in sensorimotor network occurrence probability underpin reductions in motor cortical beta power in PD.

Top left: Motor cortical 13 to 30-Hz power of people in PD (blue) is significantly reduced to healthy controls (grey) ($t(47) = 6.78$, $p < .001$). Significance was calculated with GLMs including age and sex as confounds. **Top right:** Sensorimotor network fractional occupancy of people in PD (blue) is significantly reduced compared to healthy controls (grey) ($t(47) = 4.48$, $p < .001$). Significance was calculated with GLMs contrasting fractional occupancy of all 8 states between the two groups while including age and sex as confounds and maximum t-statistic pooling to account for multiple comparisons across states. **Bottom:** Sensorimotor network fractional occupancy and beta power are positively associated ($r(49) = .75$, $p < .001$). Each dot corresponds to fractional occupancy and beta power of a single participant. Associations were calculated with a Pearson correlation.

Asterisks denote statistical significance: ** $p < 0.01$; * $p < 0.05$

Supplementary Figure 2 - State-specific absolute imaginary coherence between STN and SMA

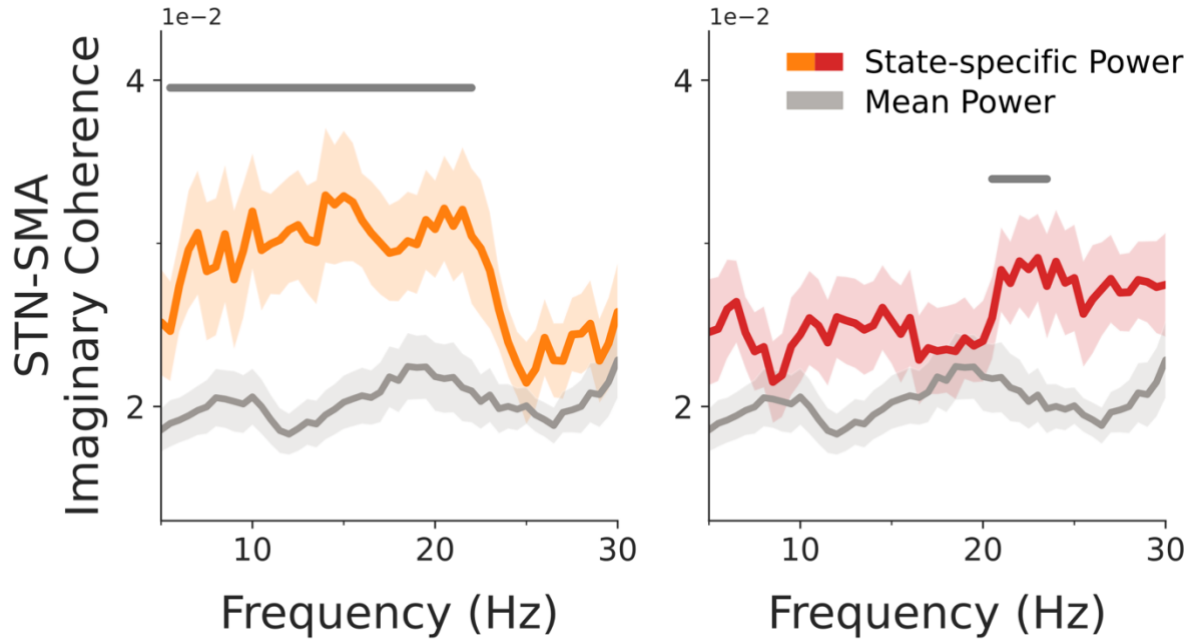

Supplementary Figure 2. State-specific absolute imaginary coherence between STN and SMA demonstrates similar connectivity patterns as state-specific coherence. Within-participant GLMs combined with cluster-based permutation testing revealed that absolute imaginary coherence between STN and SMA of the widespread activation network (orange) is significantly larger in the 5.5 to 23-Hz range than the mean absolute imaginary coherence across all states (peak frequency = 12-Hz; mean $t(24) = 3.08$, $p < .001$). Similarly, absolute imaginary STN-SMA coherence was significantly increased in the 20.5 to 24.5-Hz range during sensorimotor network occurrences (peak frequency = 23-Hz; mean $t(24) = 2.53$, $p = .023$). Grey bars indicate clusters with p-values below the Bonferroni-corrected threshold for 2 state comparisons ($p < 0.025$).

Supplementary Figure 3 – State-specific STN Beta Power

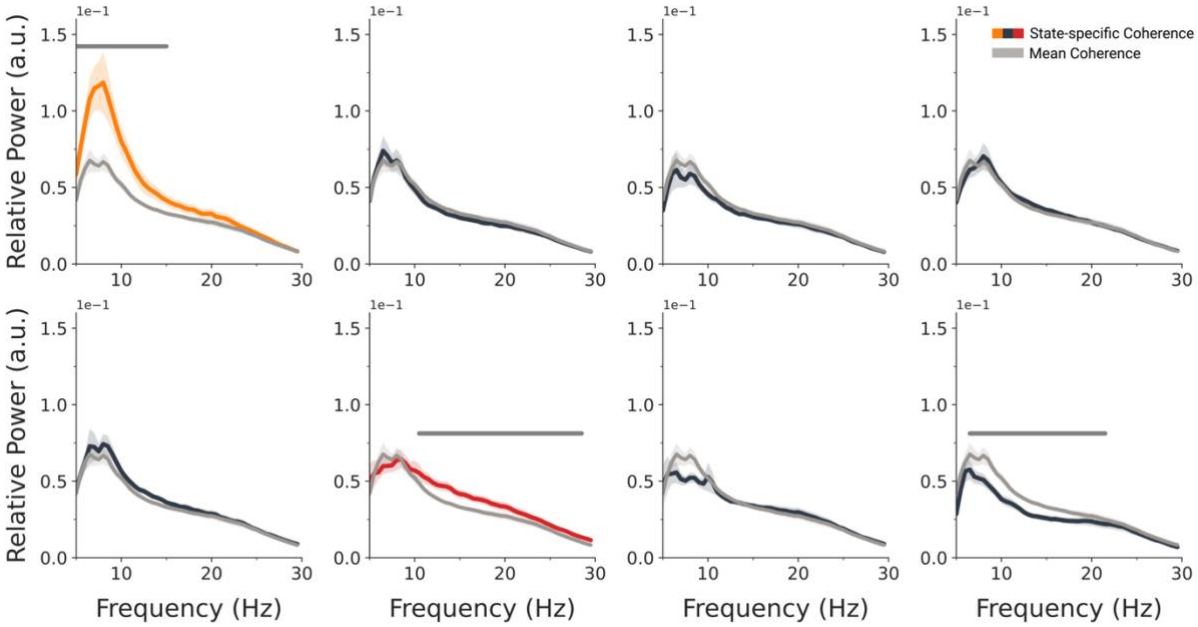

Supplementary Figure 3. STN power spectra during cortical large-scale network occurrences. State-specific STN power spectra for the widespread activation network (orange), the sensorimotor network (red), and all other networks (black) are shown alongside the time-averaged STN power spectrum across all states (grey). Cluster-based permutation testing on within-participant GLMs revealed significantly increased STN power during visits to the widespread activation network (5 to 16.5-Hz; peak = 6.5 Hz; mean t(24) = 2.91, $p <$ .001) and the sensorimotor network (9.5 to 23-Hz; peak = 14 Hz; mean $t(24) = 3.41$, $p =$ .001). In contrast, significant 6.5 to 29.5-Hz power decreases were observed for periods in which State 8 was visited (peak = 6 Hz; mean $t(24) = -4.64$, $p < .001$). Grey bars indicate clusters surviving Bonferroni correction for eight state comparisons ($p < 0.00625$).

Supplementary Figure 4 - Robustness of Effects

Running TDE-HMM analyses requires the a-priori specification of the number of states to be inferred. Since different numbers of states yield similar but slightly different network descriptions, we repeated all analyses on TDE-HMMs inferring 10 and 12 States to demonstrate that the reported findings are not limited to the choice of 8 states but are also present when selecting other numbers of states.

Repeating analysis on state-specific STN cortical-coherence for 10-State and 12-State HMMs also revealed significant increases in STN-SMA coherence for both the widespread activation and sensorimotor network, albeit with differences spreading further across the majority of frequency bands. In the 10-State HMM an significant increases in STN-SMA coherence in the 5 to 30Hz range were observed for the widespread activation network and significant increases in the 5 to 18-Hz (peak frequency = 9.5-Hz; mean $t(24) = 3.40$, $p < .001$) and 16.5 to 27.5 (peak frequency = 26.5-Hz; mean $t(23) = 3.51$, $p = .002$) range for the sensorimotor network. For the 12 State HMM, significant increases in 5 to 30Hz STN-SMA coherence were observed both during visits to the widespread activation (peak frequency = 5.5-Hz; mean $t(24) = 5.55$, $p < .001$) and sensorimotor network (peak frequency = 9.5-Hz; mean $t(24) = 3.84$, $p < .001$).

Similar to the 8 State HMM analyses of state-specific STN power spectra revealed for the 10-State HMM, significant increases in the low frequency range (6.5 to 7-Hz; peak frequency = 6.5-Hz; mean $t(24) = 1.87$, $p < .001$) for the widespread activation network and significant increases in the 10 to 23-Hz range (peak frequency = 13.5-Hz; mean $t(24) = 2.63$, $p = .002$). Low frequency increases during visits to the widespread activation network, identified from the 12-State HMM, failed to reach significance, whereas significant increases in the 10 to 22.5-Hz range (peak frequency = 18-Hz; mean t(24) = 3.84, p = .002) were replicated.

In line with findings in the 8-State HMM, widespread activation network occurrences did not significantly overlap with STN-beta bursts in the 10-State ($t(24) = 2.17$, $p = .068$) and 12-State HMMs ($t(24) = 1.97$, $p = .106$), whereas sensorimotor network occurrences did (10-State HMM: $t(24) = 3.2$, $p = .004$; 12-State HMM: $t(24) = 2.94$, $p = .008$)

Repetition of contrasts between state-specific beta power in the medication on and off conditions revealed that beta power was significantly changed only during visits to networks that do not exhibit increased levels of STN-SMA coherence, for both State-10 HMMs and 12-State HMMs. In the 10-State HMM significant decreases in state-specific beta power upon medication intake were observed for State 3 ($t(24)=3.80$, $p = .005$), State 4 ($t(24)=3.79$,

p = .005), State 9 (t(24)=3.83, p = .005), and State 10 (t(24)=3.64, p = .008). In the 12 State-HMM state-specific STN beta power was reduced for State 4(t(24)=4.07, p = .002), State 5 (t(24)=3.47, p = .011), State 10 (t(24)=3.27, p = .019), State 11 (t(24)=4.35, p = .001), State 12 (t(24)=3.75, p = .006).

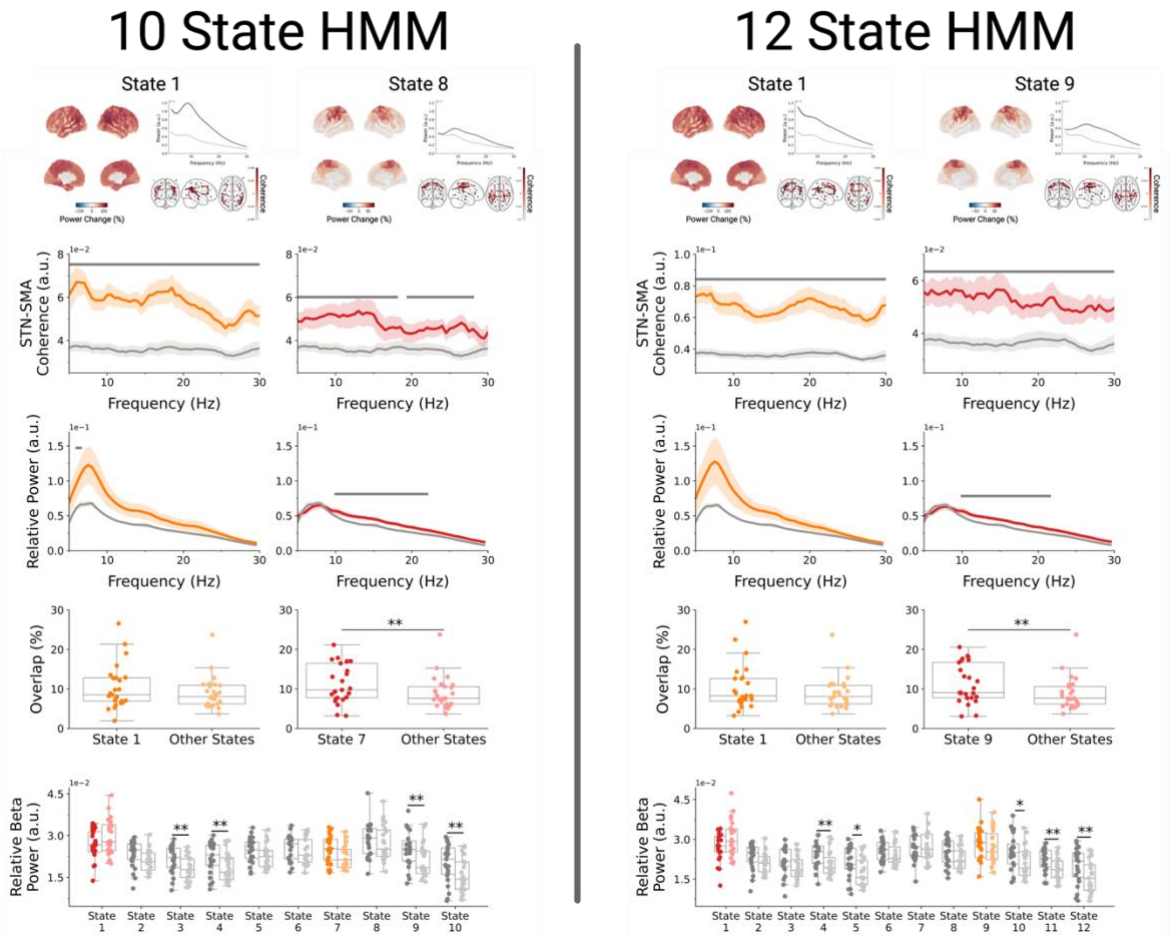

Supplementary Figure 4. 10-State and 12-State HMMs show similar patterns of change in spectral markers during widespread activation network and sensorimotor network visits. Findings for the 10-State HMM are presented on the left, and findings for the 12-State HMM on the right side. **Top row**: State descriptions of the widespread activation and sensorimotor network inferred with respective HMM. **Second row**: STN-SMA coherence for both the widespread activation network (orange) and sensorimotor network (red) is contrasted against time-average STN-SMA coherence (grey). **Third row**: State-specific STN power spectra for both the widespread activation network (orange) and sensorimotor network (red) are contrasted against the time-averaged STN power spectrum (grey). **Fourth row**: Overlap between STN beta burst and occurrences of the widespread activation network (orange) or sensorimotor network (red) are contrasted against overlaps between STN beta bursts and all

states excluding the respective state (shaded orange and shaded red). Each dot represents the overlap of a single participant. **Bottom row**: Contrast of state-specific STN beta power between medication off- (strong colours) and off-condition (shaded colours). The widespread activation network (orange) and sensorimotor network (red) are highlighted with colours. Grey bars indicate clusters surviving Bonferroni correction for eight state comparisons ($p < 0.00625$).

Asterisks denote statistical significance: ** $p < 0.01$; * $p < 0.05$

Supplementary Figure 5 – Replication HMM Overview

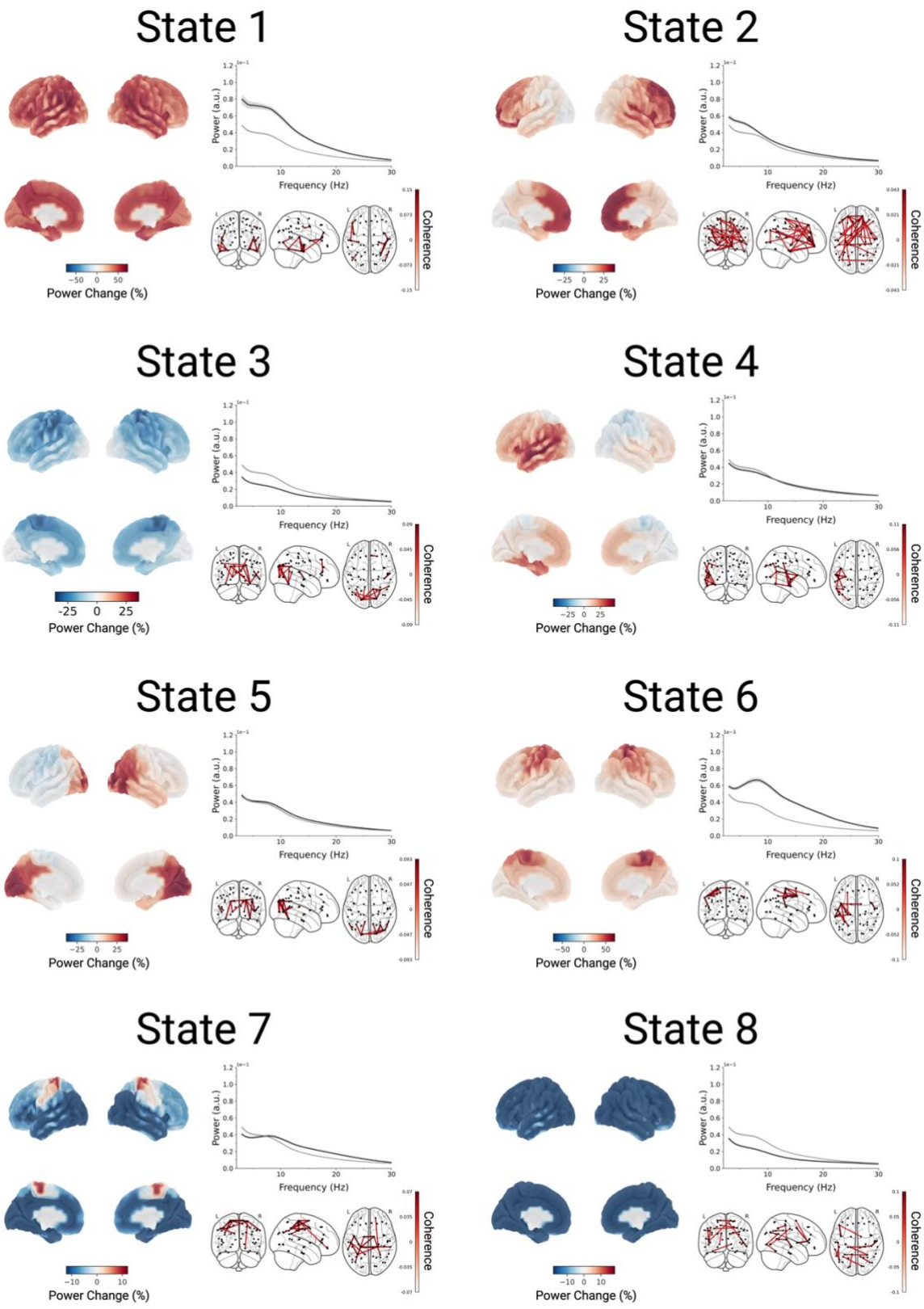

Supplementary Figure 5 Overview of dynamic large-scale cortical networks inferred from the replication dataset[1] using the TDE-HMM. Each state is presented in three panels, showing the average across scans from all participants in both the medication-off and -on conditions. **Left panel:** Deviations in 3 to 30-Hz power from the time-averaged power (calculated across all states) are projected onto the cortical surface. **Top right panel:** The state-specific motor cortical power spectrum (black) is displayed alongside the time-averaged power spectrum across all states (grey). **Bottom right panel:** Coherence networks in the 2 to 30-Hz range, thresholded at the 98th percentile, to highlight the most prominent functional connections. State 1 corresponds to the widespread activation network, and State 6 to the sensorimotor network.

Supplementary Figure 6 – State-specific STN-premotor coherence

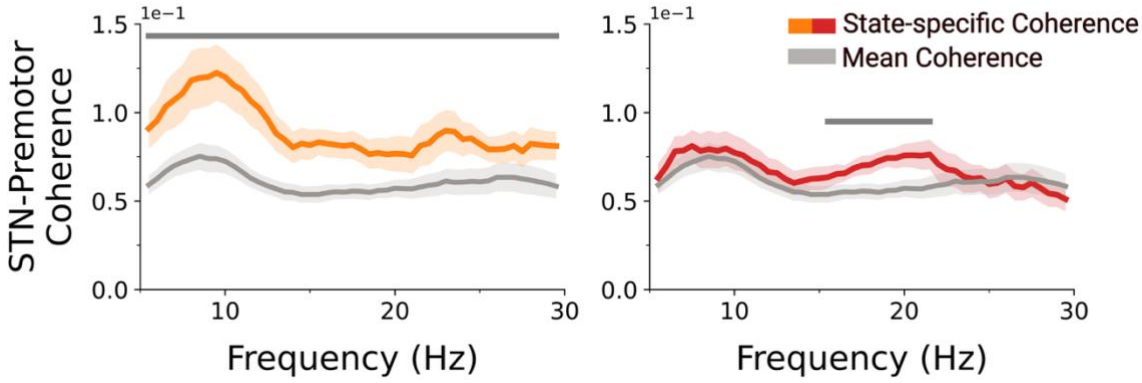

Supplementary Figure 6 State-specific STN-Premotor coherence (dark orange, dark red) is shown alongside the time-averaged coherence across all states (grey). Within-participant GLMs, combined with cluster-based permutation testing, revealed significantly increased STN-Premotor coherence during visits to the widespread activation network (State 1; orange; 5.5-29.5 Hz; peak = 16.5 Hz; mean $t(16) = 3.49$, $p < 0.001$) and the sensorimotor network (State 6; red; 15.5-21.5 Hz; peak = 19 Hz; mean $t(16) = 3.63$, $p = 0.002$).
Grey bars indicate clusters with $p < 0.00625$ (Bonferroni-corrected threshold for 8 states).